

# Overview about damage evolution of brittle rocks

Authors: Prof. Dr. habil. Heinz Konietzky & Dr. Thomas Frühwirt  
(TU Bergakademie Freiberg, Geotechnical Institute)

---

1	Introduction.....	2
2	Damage evolution under 3-dimensional compressional stress state .....	4
3	Typical fracture pattern.....	6
4	References .....	16

## 1 Introduction

Brittle rocks under loading do not only show elastic deformation but also subcritical and/or critical crack initiation and propagation (plastic deformation), which can finally also lead to macroscopic failure.

This chapter considers damage evolution observed during typical lab tests and reveals the main mechanisms. Damage evolution is a complicated process, which begins at the micro-level (atomic level to grain-size level) and ends with the development of single or several macroscopic fractures, which split the sample into several pieces. The damage evolution depends on several parameters, like initial damage state of the sample, loading velocity, environmental conditions, sample shape and size, boundary conditions etc.

Damage evolution is a process in time and space and difficult to observe in detail. Damage development of lab samples under loading can be monitored by seismic pulsing or tomography, acoustic emission monitoring (e.g. Zaho et al. 2015) or computer tomography. Also, detailed deformation measurements (e.g. volumetric response and dilation, respectively) with separation of elastic and plastic parts give indications of damage evolution (e.g. Hoek & Martin 2014, Diederichs et al. 2004, Cai et al. 2004).

In general two steps of damage can be distinguished as shown in Fig. 1:

- Pre-failure range
- Post-failure range

In the post-failure range strain softening is the typical behavior of brittle rocks. Strain hardening is only observed for certain soft rocks, to some extent for salt rocks and some soil-like materials.

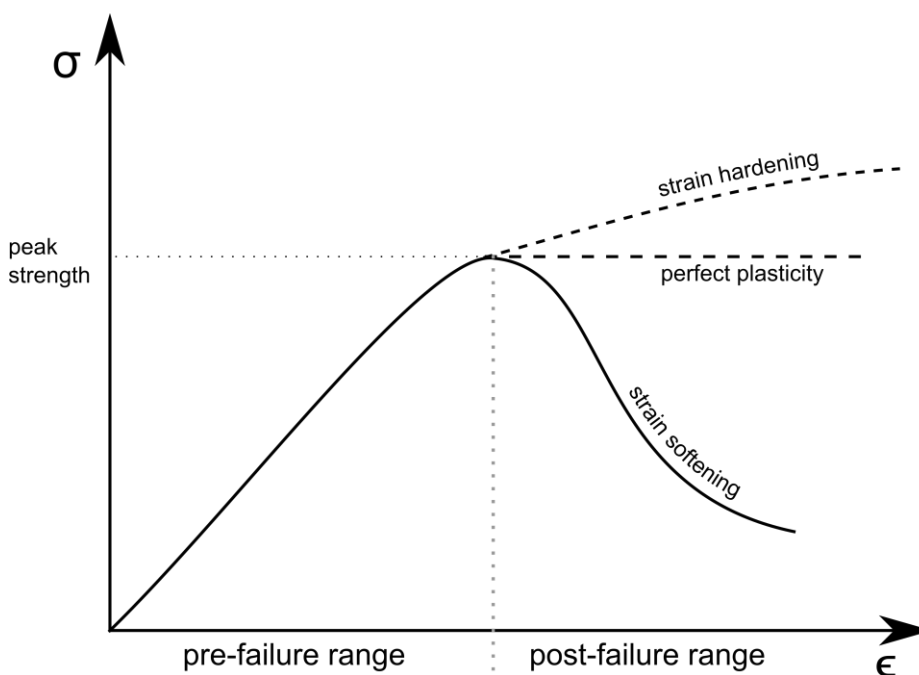


Fig. 1: General stress strain behavior for rock/soil samples under compression

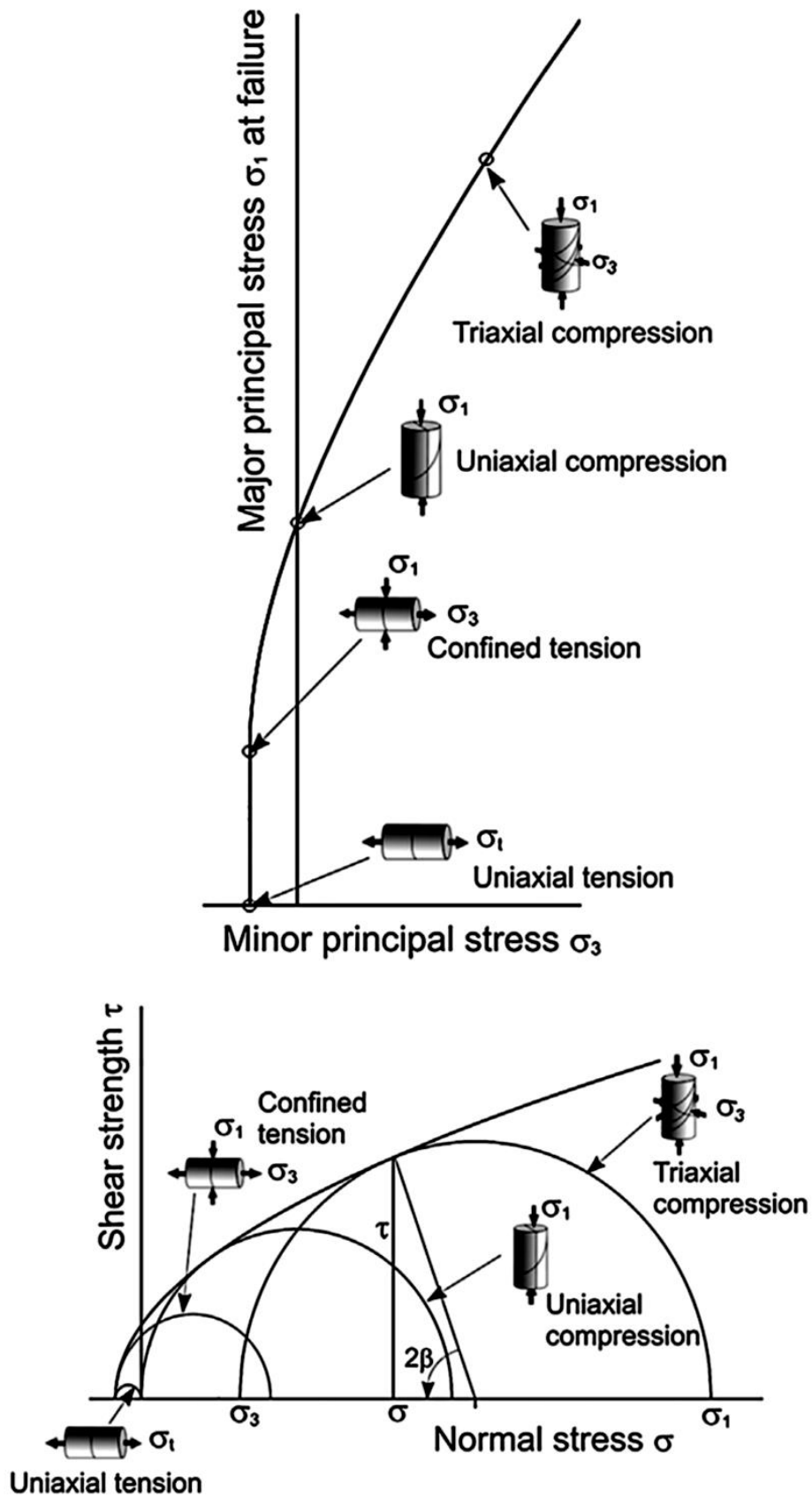


Fig. 2: Overview plot of different loading situations [Hoek & Martin 2014]

## 2 Damage evolution under 3-dimensional compressional stress state

The most typical loading situation in rock engineering is the 3-dimensional compressional stress state including biaxial and uniaxial compression as special cases like observed at unsupported surfaces of underground excavations.

Damage evolution of brittle rocks comprises the initiation, propagation and coalescence of microcracks until a macroscopic fracture is formed which finally leads to total failure. Several distinguished stress levels can be defined (see also Fig. 3 and 4):

- Crack closure stress level:  $\sigma_{cc}$
- Crack initiation stress level:  $\sigma_{ci}$
- Crack damage stress level:  $\sigma_{cd}$
- Peak stress level:  $\sigma_{peak}$

This process can be characterized by the following stages (see also Fig. 3 and 4):

- 1) First phase (low stress level) is characterized by crack closure combined with volumetric compaction. Material behavior is nearly elastic.
- 2) Crack initiation starts between app. 30% and 50% of peak stress and is characterized by crack initiation stress  $\sigma_{ci}$  (see also Fig. 5). Stable crack growth is typical for a stress level between  $\sigma_{ci}$  and  $\sigma_{cd}$ . AE and dilation are starting at  $\sigma_{ci}$ .
- 3) Fracture coalescence starts at about 70% to 80% of peak stress and is characterized by crack damage stress  $\sigma_{cd}$ .
- 4) Fracture coalescence takes place in the range between  $\sigma_{cd}$  and peak stress  $\sigma_{peak}$ . At this phase unstable crack growth starts.
- 5) Final localization, shear banding and macroscopic fracture development takes place in the post-failure region after  $\sigma_{peak}$  has been reached. This phase is characterized by massive unstable crack growth and rock desintegration.

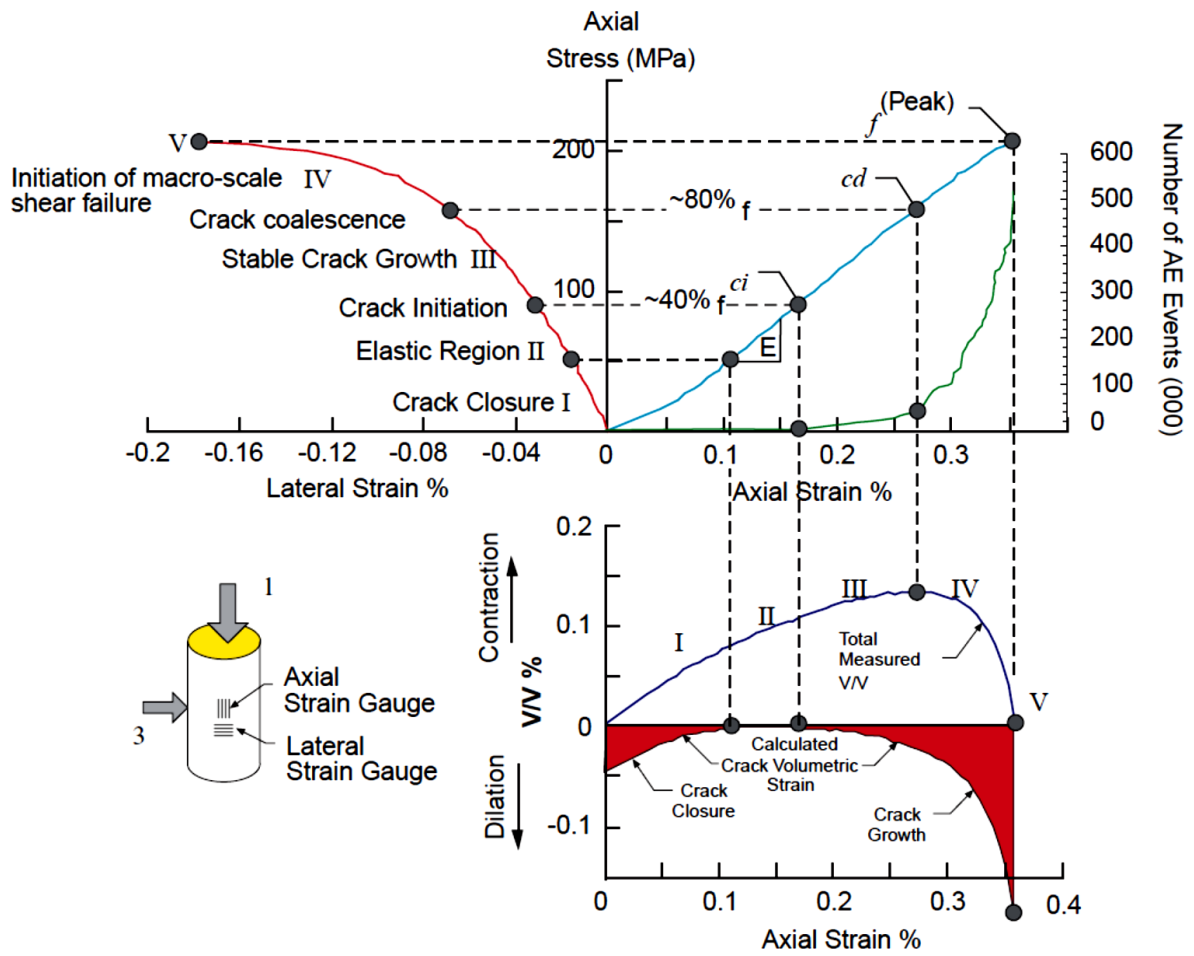


Fig. 3: Illustration of damage stages in stress strain diagrams [Cai et al. 2004]

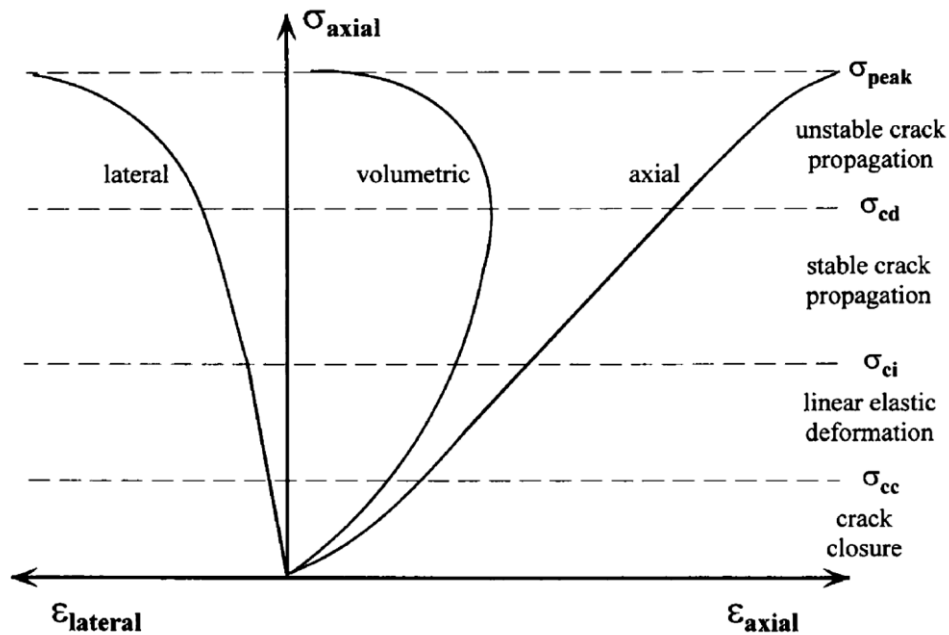


Fig. 4: Triaxial compression test: Axial, lateral and volumetric deformation vs. axial stress [Diederichs et al. 2004]

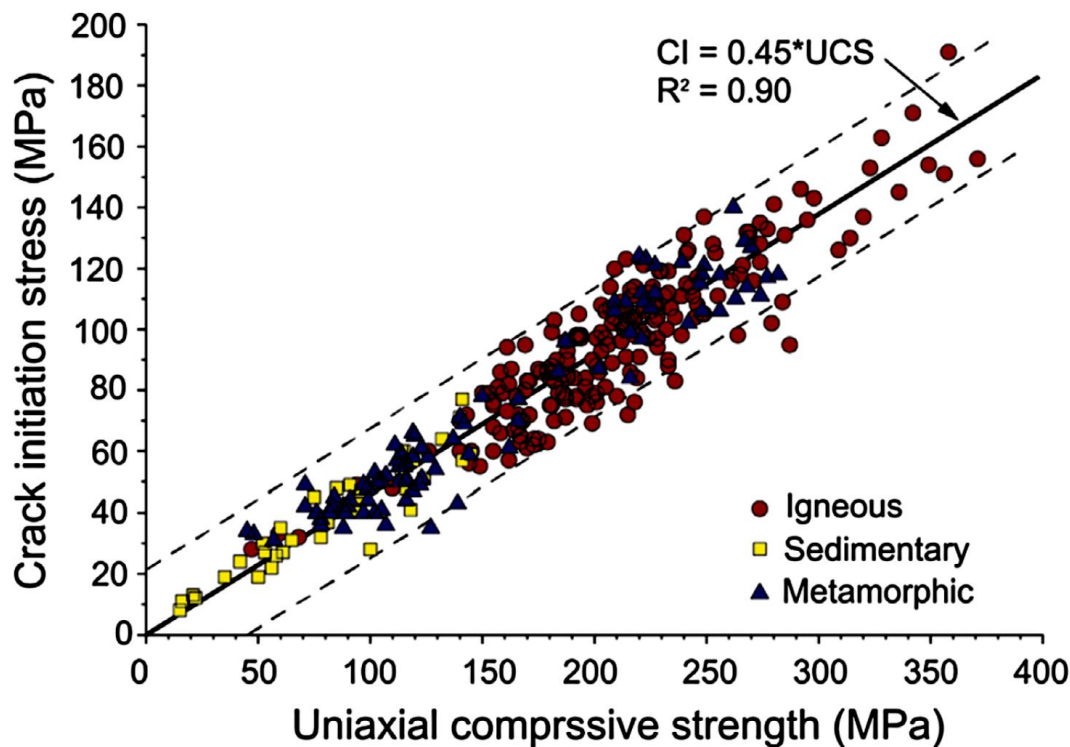


Fig. 5: General relation between crack initiation stress and UCS [Hoek & Martin 2014]

### 3 Typical fracture pattern

Three most typical loading situations can be distinguished (see also Fig. 2):

- Uniaxial compression
- Uniaxial tension
- 3-axial compression

Besides these typical loading situations further situations exist, like special biaxial loading conditions as well as 3-axial loading conditions with compressional and extensional components. This chapter considers only the three above mentioned simple loading situations.

Under uniaxial tension only one single tensile fracture develops starting at the weakest point and propagating perpendicular to the applied tensile load (Fig. 6).

Under uniaxial compression four different final fracture pattern can be considered as typical:

- Vertical splitting (Fig. 7)
- Single inclined shear crack (Fig. 8)
- Conjugated shear fracturing creating a double cone shape (Fig. 9)
- Mixed-mode shear-tensile fracturing (Fig. 10)

Which type of fracture develops is mainly depending on the orientation of the microcracks (anisotropy in strength) of the sample in relation to the loading direction. One

typical example is slate: If the bedding plane is parallel to the loading direction, vertical splitting is observed (see Fig. 7 above); if loading direction is perpendicular to orientation of microcracks, mixed-mode shear-tensile fracturing will occur (see Fig. 10 below). Under 3-dimensional compression macroscopic shear fracturing dominates as illustrated in Fig. 11.

Fig. 12 shows a schematic illustration of typical rock failure modes observed under uniaxial compression. Basu et al. [2013] found, that axial splitting dominates for rocks with lower UCS values, whereas shearing including multiple fracturing dominates for rocks with higher UCS. For rocks with pronounced anisotropy failure develops mostly along planes of weakness (foliation).



Fig. 6: Uniaxial tension tests: broken samples (gneiss-concrete-interface above, sandstone below) showing clearly developed tensile crack [RML 2016]



Fig. 7: Uniaxial compression test: vertical splitting (slate above, granite below) [RML 2016]



Fig. 8: Uniaxial compression test: single include shear fracture (gneiss above, gneiss below) [RML 2016]

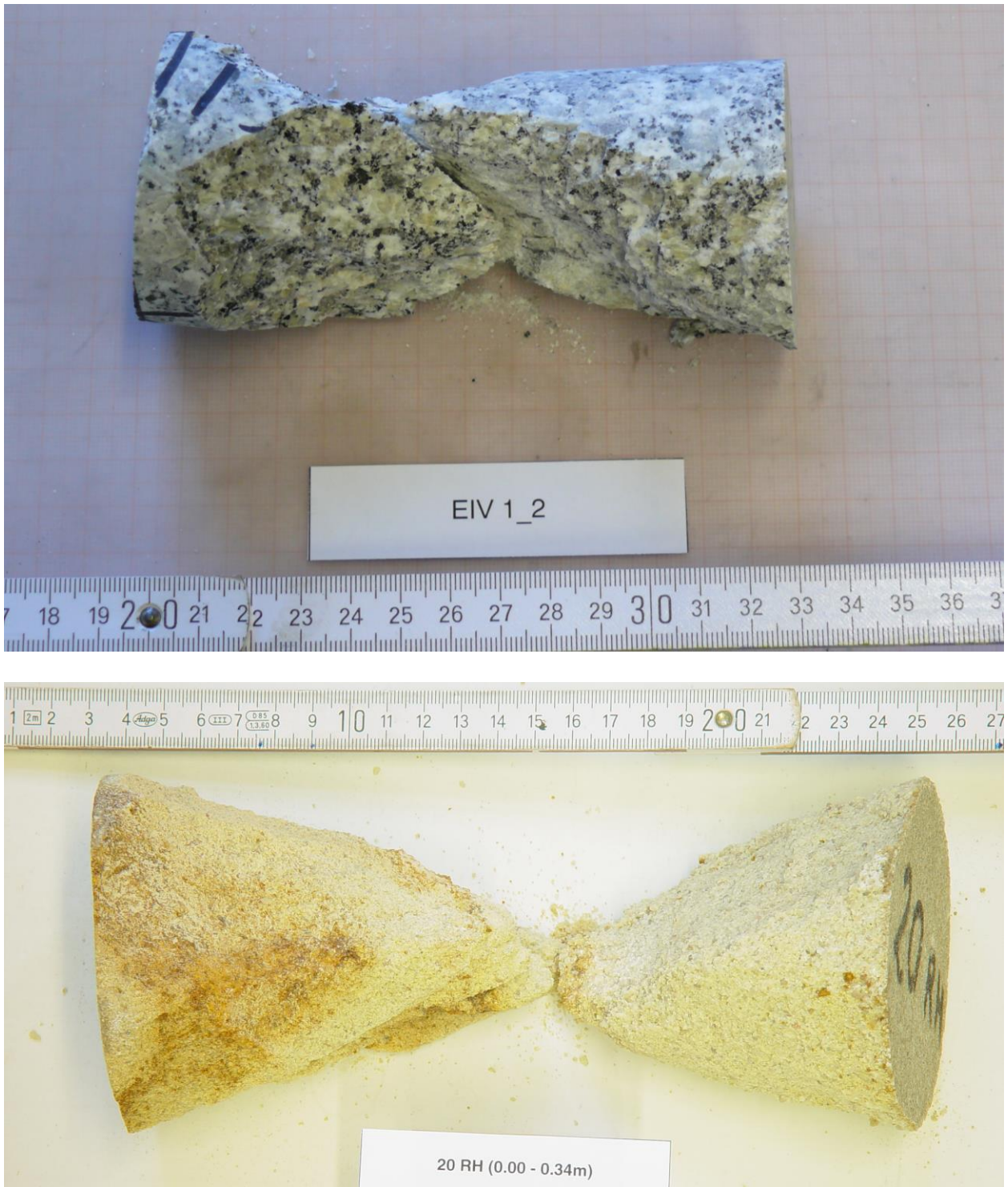


Fig. 9: Uniaxial compression test: conjugated shear fracturing creating a double cone shape (granite above, sandstone below) [RML 2016]



Fig. 10: Uniaxial compression test: mixed-mode shear-tensile fracturing (gneiss above, slate below) [RML 2016]



Fig. 11: Triaxial tests: single shear fractures as final fracture pattern, granite samples tested at different confining pressures (10, 20 and 30 MPa)

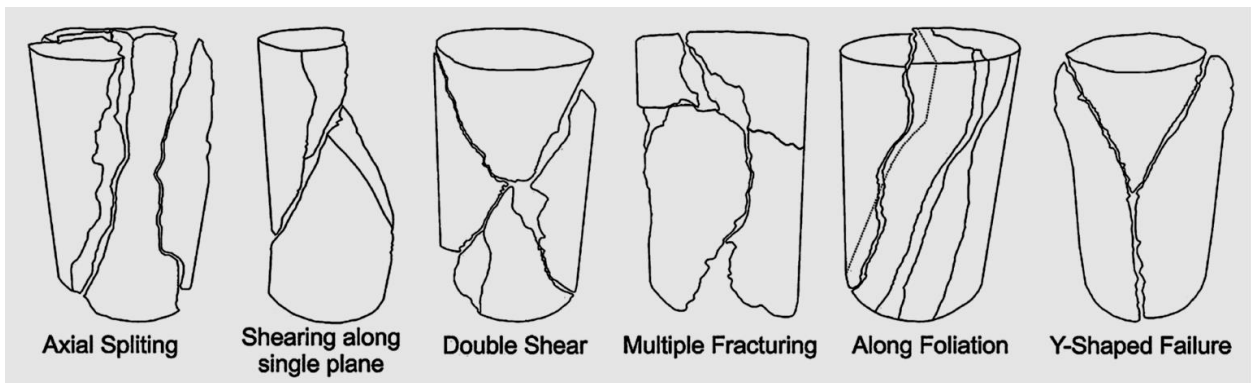


Fig. 12: Schematic representation of typical failure modes [Basu et al. 2013]

The damage evolution can be simulated using continuum (e.g. Li & Konietzky 2015, Li et al. 2016, Li & Konietzky 2017) or discontinuum (e.g. Chen et al. 2016, Tan et al. 2015, Tan et al. 2016) mechanical approaches. Fig. 13 illustrates how initial microcrack orientations can influence the macroscopic fracture pattern: (a) shows vertical splitting, (b) single shear crack and (c) conjugated shear fracturing combined with mixed-mode fracturing. Fig. 14 compares final fracture pattern for a sample with uniform microcrack orientation under uniaxial tension and uniaxial compression.

Besides continuum based simulations also discontinuum based approaches (Discrete Element Method or particle based approaches) can be used to simulate crack initiation and propagation as shown in Fig. 15. Corresponding lab test results are shown in Fig. 16, 17 and 18. The indices  $b_1$ ,  $b_2$  and  $b_3$  indicate the peak loading stages ( $\sigma_1$  reaches the maximum value) under  $\sigma_2=10, 20, 30$  MPa, respectively, and the indices  $c_1$ ,  $c_2$  and  $c_3$  are the reversal points in volumetric strain. Fig. 16 shows the energy balance deduced from strain and stress measurements. The difference between total boundary work and elastic strain energy is the dissipated energy, which comprises heat generation, fracture energy as well as seismic energy as main components. Based on either the actual stiffness or the energy balance, a damage value (0=undamaged, 1=total

damage) is defined. Such analysis allows to observe the overall damage evolution with increasing loading.

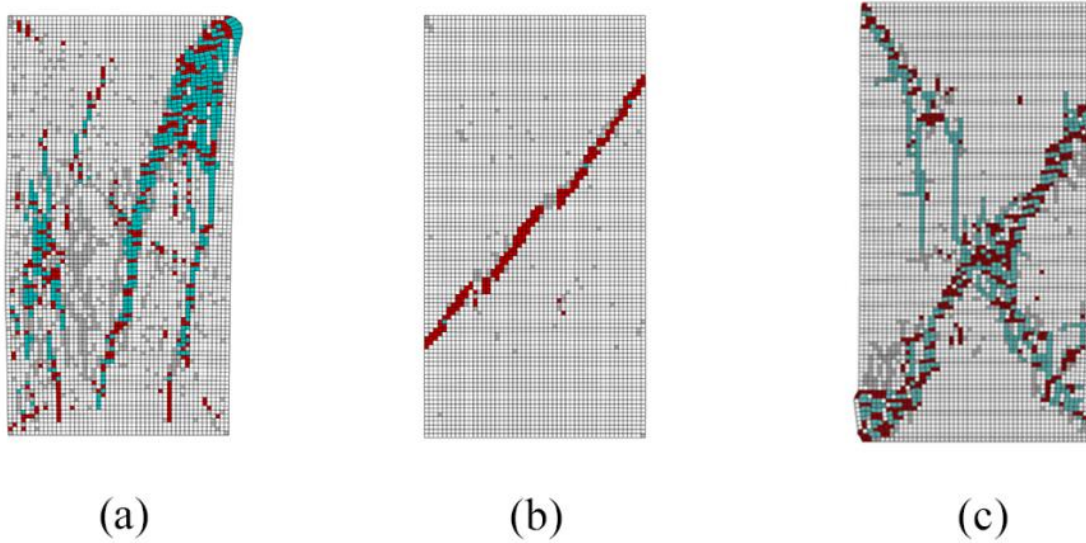


Fig. 13: Typical fracture pattern for uniaxial compression tests based on continuum mechanical simulation (a: microcrack orientation follows normal distribution with mean vertical direction; b: microcrack orientation follows normal distribution with mean direction of 60°; c: microcrack orientation follows uniform distribution – red: microscopic shear fracturing, blue: microscopic tensile fracturing) [Li & Konietzky, 2017]

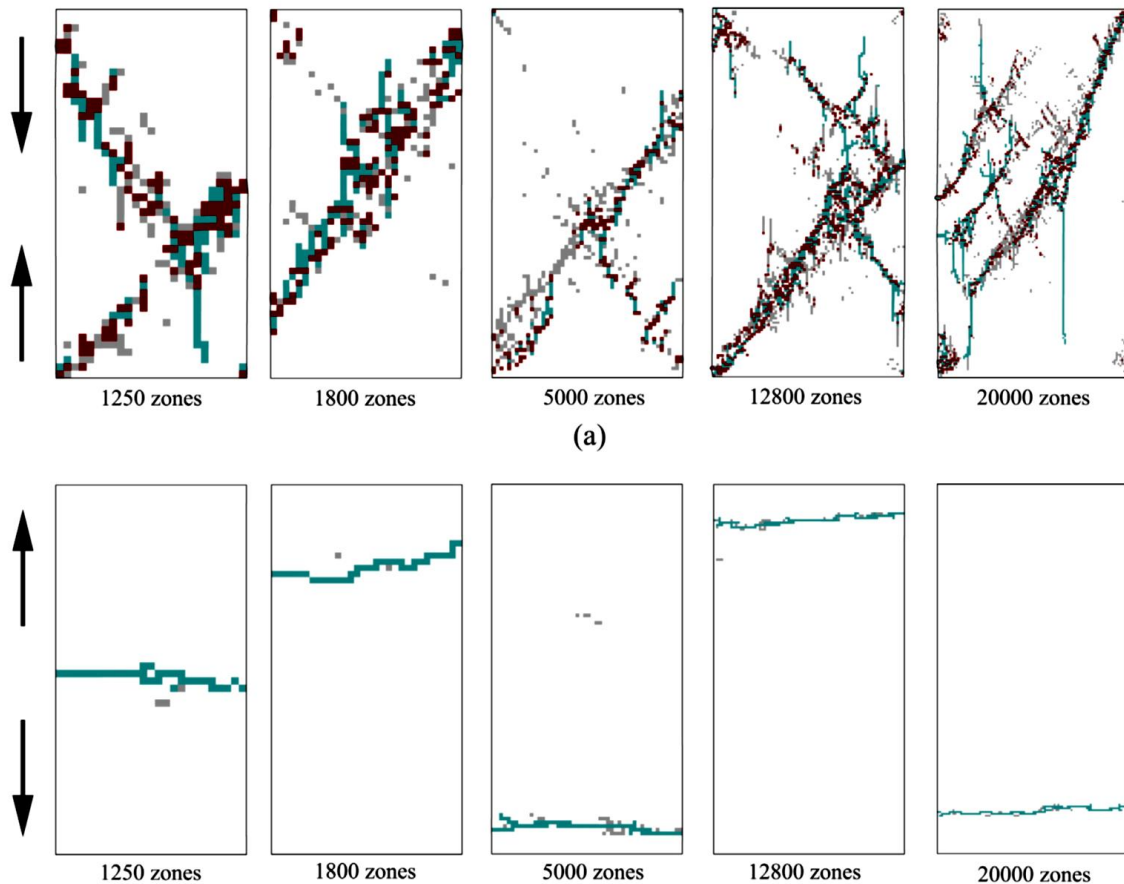


Fig. 14: Fracture pattern for uniaxial compression (above) and uniaxial tension (below) test assuming uniform microcrack distribution – red: shear cracks, blue: tensile cracks [Li & Konietzky 2016]

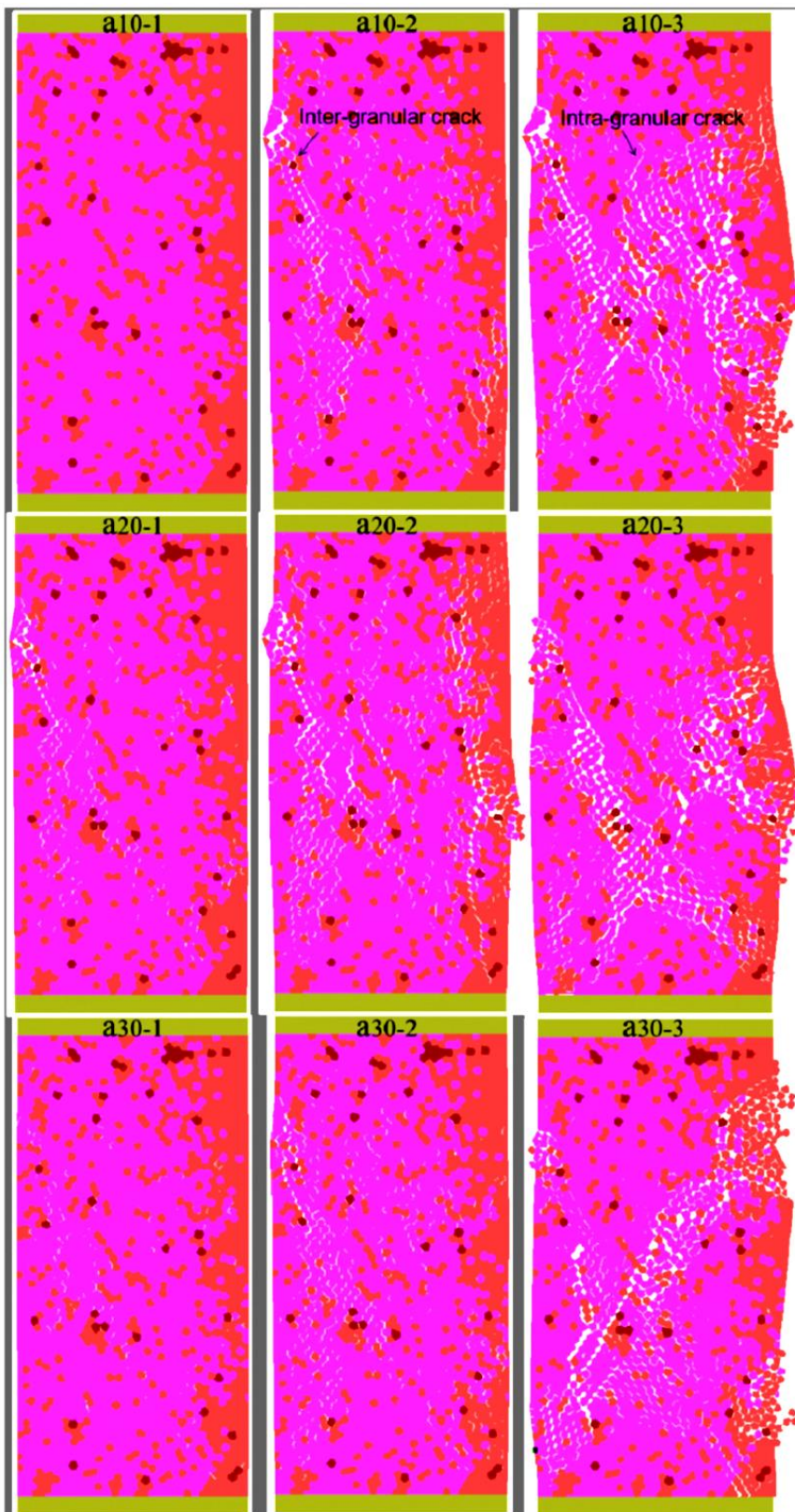


Fig. 15: DEM based simulation of damage evolution in granite (3-axial loading with 10, 20 and 30 MPa confining pressure) [Chen et al. 2016]

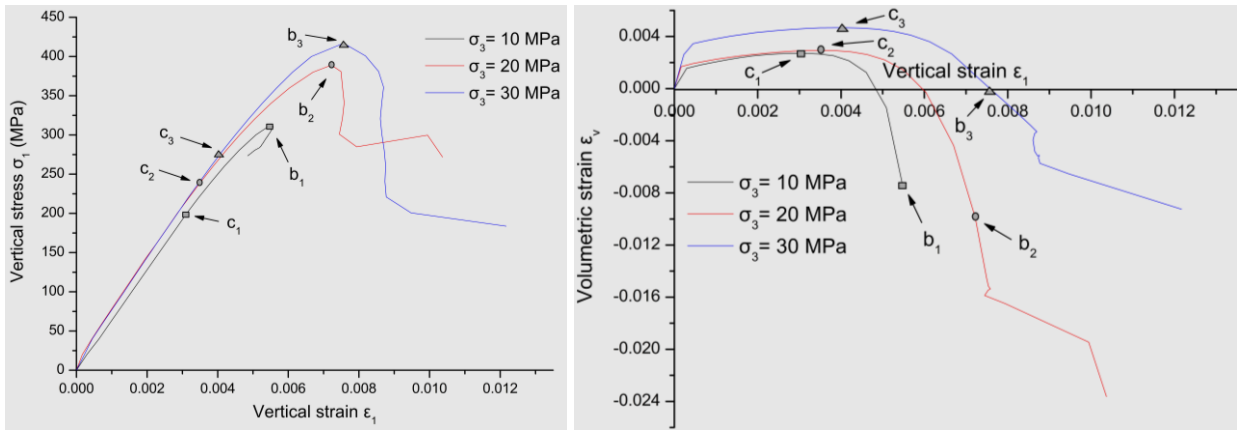


Fig. 16: Triaxial tests of granite: stress strain curves at confining pressures of 10, 20 and 30 MPa [Chen et al. 2016]

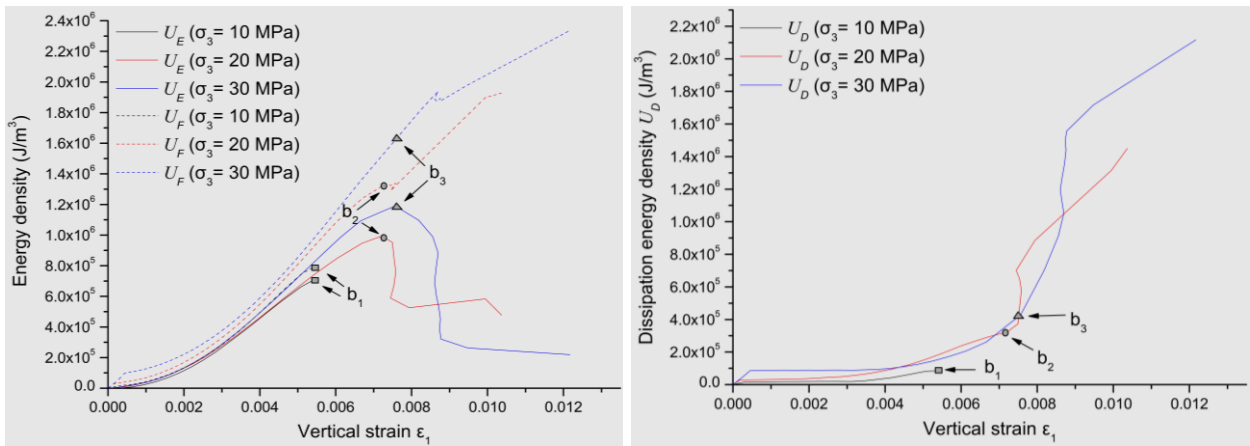


Fig. 17: Triaxial tests of granite: energies vs. strain [Chen et al. 2016]

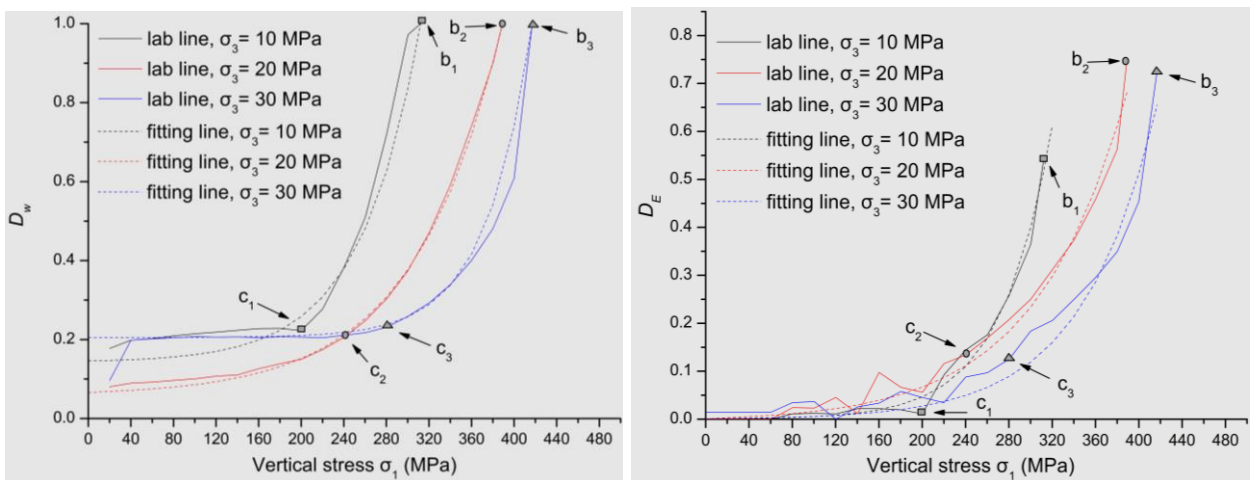


Fig. 18: Triaxial tests of granite: damage parameters vs. strain [Chen et al. 2016]

## 4 References

- Basu, A. et al. (2013): Rock failure modes under uniaxial compression, Brazilian, and point load tests, *Bull. Eng. Geol. Environ.*, 72: 457-475
- Cai, M. et al. (2004): Generalized crack initiation and crack damage stress thresholds of brittle rock masses near underground excavations, *Int. J. Rock Mech Min. Sci.*, 41: 833-847
- Chen, W. et al. (2016): Pre-failure damage analysis for brittle rocks under triaxial compression, *Computers and Geotechnics*, 74: 45-55
- Diederichs, M.S. et al. (2004): Damage initiation and propagation in hard rock during tunneling and the influence of near-face stress rotation, *Int. J. Rock Mech Min. Sci.*, 41: 785-812
- Hoek, E. & Martin, C.D. (2014): Fracture initiation and propagation in intact rock – A review, *J. Rock Mechanics and Geotechnical Engineering*, 6: 287-300
- Li, X., Konietzky, H. (2015): Numerical simulation schemes for time-dependent crack growth in hard brittle rock, *Acta Geotechnica*, 10: 513-531
- Li, X., Konietzky, H. & Li, X. (2016): Numerical study on time dependent and time independent fracturing processes for brittle rocks, *Engineering Fracture Mechanics*, 163: 89-107
- Li, X. & Konietzky, H. (2017): Relation between fracture modes and initial microcrack distribution, in preparation
- Nicksiar, M. & Martin, C.D. (2013): Crack initiation stress in low porosity crystalline and sedimentary rocks, *Engineering Geology*, 154: 64-76
- RML (2016): Rockmechanical laboratory, Geotechnical Institut, TU Bergakademie Freiberg
- Tan, X., Konietzky, H., Chen, W. (2016): Numerical simulation of heterogeneous rock using discrete element model based on digital image analysis, *Rock Mech Rock Eng.*, 49: 4957-4964
- Tan, X. et al. (2015): Brazilian tests on transversely isotropic rocks: laboratory testing and numerical simulations, *Rock Mech Rock Eng.*, 48: 1341-1351
- Tang, C. & Hudson, J.A. (2010): *Rock failure mechanisms*, CRC Press, 319 p.
- Zhao, X.G. et al. (2015): Objective determination of crack initiation stress of brittle rocks under compression using AE measurements, *Rock Mechanics Rock Engineering*, DOI 10.1007/s00603-014-0703-9